Noncritically phase-matched second-harmonic-generation chalcopyrites based on $CdSiAs_2$ and $CdSiP_2$

Walter R. L. Lambrecht and Xiaoshu Jiang
Department of Physics, Case Western Reserve University, Cleveland, Ohio 44106-7079, USA
(Received 24 November 2003; revised manuscript received 13 April 2004; published 21 July 2004)

The indices of refraction as a function of wavelength are calculated from first-principles band structure calculations for $CdSiAs_2$ and $CdSiP_2$. Both are found to have negative birefringence in good agreement with experimental data. Examining the birefringence data among various chalcopyrites suggests a linear dependence of birefringence on c/a and thus on tetragonal strain. First-principles calculations confirm this expectation and give $d\Delta n/d\eta = 1.7$ for $CdSiAs_2$ and 2.3 for $CdSiP_2$ with η the uniaxial tetragonal strain. Estimates are made of the mid infrared dispersion based on the calculations combined with experimental data on midinfrared optical absorption. Phase matching curves are calculated based on these results as function of strain in $CdSiAs_2$ and in mixed $CdSi(As_{1-x}P_x)_2$ alloys. Uniaxial strains of order 1% or mixing with $CdSiP_2$ are required for $CdSiAs_2$ to provide noncritial phase matching in the midinfrared range. Combined with the relatively high $\chi^{(2)}$ of these materials, they are concluded to be potentially competitive nonlinear optical materials.

DOI: 10.1103/PhysRevB.70.045204 PACS number(s): 78.20.Fm, 42.65.Ky

I. INTRODUCTION

Chalcopyrite semiconductors have not only high second-order optical susceptibilities $\chi^{(2)}$ but also birefringence which allows for angular tuning of the phase matching. In negative birefringent crystals a condition known as noncritical phase matching (NCPM) is highly desirable because it optimizes the effective conversion coefficient, given by

$$\chi^{(2)}_{\text{eff}} = \sin\,\theta\chi^{(2)}_{zxy}, \tag{1}$$

for type-I (i.e., *ooe*) second harmonic generation (SHG) in chalcopyrites. Indeed it corresponds to $\theta = 90°$, where θ is the angle between the beam and the optical axis. Furthermore, since under these conditions the beams propagate along a crystallographic axis, walk off is avoided and the phase matching is less sentitive to beam divergence, thus increasing the overall efficiency. In order to achieve NCPM for a given target wavelength, the material's birefringence must be adjusted. This can be done by adjusting the composition of an alloy between semiconductors with different birefringence. This concept has previously been proposed for $AgGa(Se_{1-x}Te_x)_2$ alloys.[1]

The II-IV-V_2 chalcopyrites generally have larger $\chi^{(2)}$ than the I-III-VI_2 family.[2,3] They also have a better thermal conductivity,[4,5] which translates into a higher laser-damage-threshold and higher allowable maximum power. However, both $CdGeAs_2$ and $ZnGeP_2$, the two II-IV-V_2 chalcopyrites primarily under development, have positive birefringence, excluding NCPM. The question arises whether a II-IV-V_2 chalcopyrite semiconductor exists with negative birefringence from which to design NCPM alloys with high effective $\chi^{(2)}$. This question is critically examined here using a combination of literature data on chalcopyrites supplemented by first-principles calculations.

The available literature data[5,6] suggest that birefringence varies linearly with c/a ratio at least within a given closely related family of materials, e.g., the various AgGa-VI_2 compounds or the various Zn-(Si,Ge)-$(As,P)_2$ compounds or Cd-(Si,Ge)-$(As,P)_2$ compounds. This is illustrated in Fig. 1 and is to be expected because both quantities are a measure of the anisotropy. The only presently known negative birefringent II-IV-V_2 chalcopyrites are $CdSiP_2$ and $CdSiAs_2$. Furthermore, however, this linear dependence on c/a suggests that birefringence should depend linearly on tetragonal strain, which might offer new opportunities for tuning the birefringence to any desired value.

In this paper we check this empirical prediction by using first-principles calculations of the birefringence in $CdSiAs_2$ and $CdSiP_2$. We also confirm and quantify the linear dependence of birefringence on strain. The computational method used for these birefringence calculations is described in Sec. II. We present our results on the birefringence in $CdSiAs_2$ and $CdSiP_2$ in Sec. III A. In order to evaluate the possibilities for phasematching, we also need to know the dispersion in the mid infrared range. Our calculations are expected to give a reasonable description of the dispersion in the region where the dispersion effects due to the electronic transitions

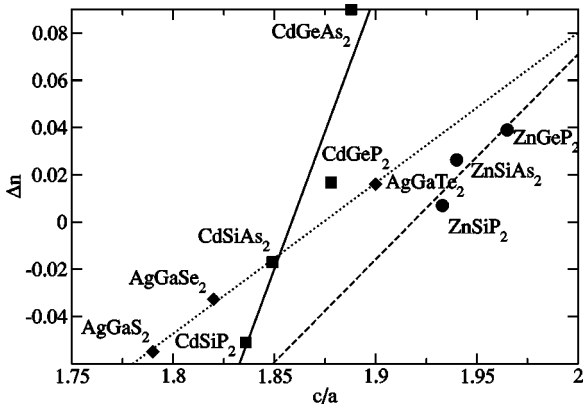

FIG. 1. Birefringence as a function of c/a for various chalcopyrites. Experimental data taken from Refs. 5 and 6. Least squares approximations to the data within a chosen family give the straight lines.

dominate over those from the phonon effects. The Sellmeyer equation provides a convenient way to parametrize the index of refraction as function of wavelength. It describes the optical absorption from electronic transitions and from phonon excitation each by a single pole. We thus use our first-principles calculated dispersion to extract the Sellmeyer coefficients *A*, *B*, and *C* related to the electronic optical transitions. These results are presented in Sec. III B. However, the phonon related dispersion is important in the midinfrared. By careful examination of the available experimental data on chalcopyrites, we show that the *E* Sellmeyer parameter which represents the phonon effects by a single pole can be estimated from the TO phonon frequency while the *D* parameter is effectively independent of material. This allows us to make estimates of the *D* and *E* parameters for $CdSiAs_2$ and $CdSiP_2$. Finally, we are then in a position to discuss the phasematching opportunities in $CdSiAs_2$ and $CdSiP_2$, as discussed in Sec. III C. We show that strains of order 1% in $CdSiAs_2$ are necessary to provide phase matching and more particularly NCPM in the useful ranges in the midinfrared. On the other hand, $CdSiP_2$ has sufficient birefringence to provide phasematching and furthermore it could be tuned by alloying with $CdSiAs_2$. The strains of 1% are substantial but by calculating the relevant elastic constant we show that it corresponds to stresses $\sigma < 1$ GPa, which are feasible based on literature data.[7] The second harmonic coefficients of these materials which were calculated in previous work[2] are compared with those of other materials presently in use to evaluate the potential of these materials in Sec. III D. We conclude that these materials are potentially competitive NLO materials.

II. COMPUTATIONAL METHOD

First-principles calculations of the indices of refraction were performed based on density functional band structure calculations. The linear muffin-tin orbital method (LMTO) is used in the atomic-sphere approximation (ASA)[8] and the local-density approximation (LDA) is used for exchange and correlation.[9] After converging the potential to self-consistency using a well converged regular $6\times6\times6$ **k**-point mesh, the imaginary part of the optical dielectric function $\varepsilon_2(\omega)$ is obtained by summing over interband transitions neglecting local field and excitonic effects as described in Ref. 10. We calculated $\varepsilon_2(\omega)$ up to about 27 eV. In fact, $\varepsilon_2(\omega)$ is already negligibly small above 12 eV. Our calculation includes 14 conduction bands and the 22 uppermost valence bands, i.e., the anion *p*-like bands, and Cd *d* bands, although the latter made little or no contribution. The tetrahedron method with a large $20\times20\times20$ regular **k**-point mesh was used to perform the Brillouin zone integrals. An energy mesh of 1200 energy points was used between 0 and 27 eV. Based on earlier experience with calculation of optical properties, e.g., in Ref. 10, we know that these computational parameters are sufficient to obtain the real part $\varepsilon_1(\omega)$ by Kramers-Kronig transformation. Finally the complex index of refraction is obtained from $n(\omega)+ik(\omega)=\sqrt{\varepsilon_1(\omega)+i\varepsilon_2(\omega)}$. Here we show results only for $n(\omega)$ for $\hbar\omega$ below the band gap although we did calculate both up to 27 eV. Since the well-known LDA underestimate of the band gap can significantly affect the calculated indices of refraction, a rigid shift of the conduction band is introduced simply by shifting the $\varepsilon_2(\omega)$ by the band-gap correction before calculating $\varepsilon_1(\omega)$ and $n(\omega)$. This is equivalent to a scissor's shift accompanied by a renormalization of the momentum optical matrix elements.[11]

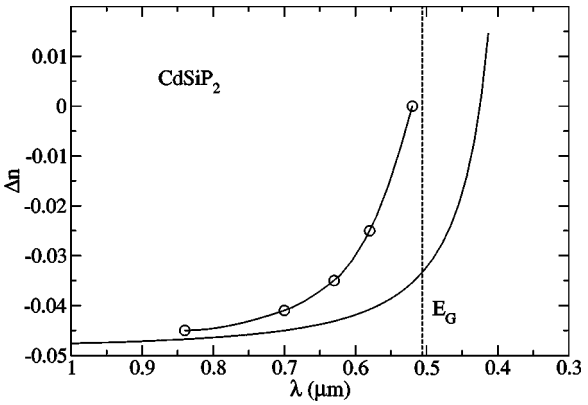

FIG. 2. Birefringence of $CdSiP_2$, solid line theory, circles with spline interpolation, experimental data from Itoh *et al.* (Ref. 12).

The absolute indices of refraction may still show a fairly large systematic error from the experiments because of the lack of local field effects in our calculations. This effect may lead up to a typical 20% underestimate of the static index of refraction. However, one may expect that this is a more or less constant error and hence the birefringence, i.e., the difference between the indices of refraction between two polarization directions should have a much smaller error of a few percent at most. The same is true for the dispersion, that is, the variation of the indices of refraction with frequency. The overall reliability of the present method to calculate birefringence has been demonstrated in earlier work.[2] In particular, it was found there that the calculated birefringence of $CdGeAs_2$ and $ZnGeP_2$ agree with the experimental values to better than 10% for wavelengths sufficiently far above the phonon-absorption range and sufficiently below the band gap. Near the band gap defect absorption effects tend to increase the birefringence faster than the calculations predicted. Also, while the calculated birefringence decreases to a nearly constant value for increasing wavelengths in the mid to far infrared, the experiments show an increase when the phonon absorption range is approached.

III. RESULTS

A. Birefringence

We first show our results for the birefringence in $CdSiP_2$. The calculated birefringence as function of wavelength is shown in Fig. 2 compared to the experimental data from Itoh *et al.*[12]

One may notice that the experimental birefringence increases faster when approaching the band gap than the calculated one. This may well be a result of defect or exciton absorption below the band gap, as was also found to be the case for $CdGeAs_2$.[2] Our calculated value for the static value

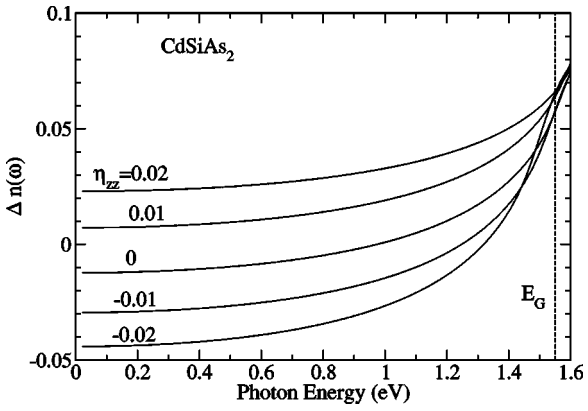

FIG. 3. Birefringence as a function of photon energy for $CdSiAs_2$ for different uniaxial strains η along the c axis.

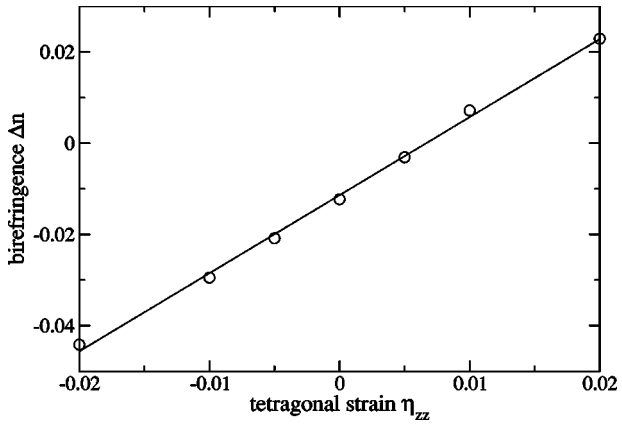

FIG. 4. Calculated long-wavelength value of the birefringence as a function of strain for $CdSiAs_2$.

of the birefringence for $CdSiP_2$ is $\Delta n = -0.049 \pm 0.006$. This calculation uses experimental lattice constants and the experimental value for the internal structural parameter for the chalcopyrite structure from Ref. 5. A gap correction of 1.28 eV was used assuming an experimental gap of 2.45 eV. Values ranging from 2.08 to 2.45 eV have been reported[5] for the gap of $CdSiP_2$. We checked that the birefringence is not very sensitive to the choice of gap correction in this case because the LDA gap is sufficiently large to start with. It varies by less than 0.001 even when using the LDA gap. We checked that the birefringence is also insensitive to the internal structural parameter. Using a value of $u=0.2923$ obtained from a full-potential (FP) LMTO (Ref. 13) energy minimization instead of the experimental value $u=0.2967$ changed the result to -0.043. The experimental value used in Fig. 1 from Ref. 5 is -0.051 and corresponds to $\lambda=2.06$ μm and $T=300$ K. At the longest wavelength considered 0.82 μm in Itoh *et al.*,[12] the birefringence seems to flatten out at a value of about -0.045. In other words, our uncertainty seems comparable to the experimental one and excellent agreement is obtained between both.

The results for the birefringence in $CdSiAs_2$ are shown in Fig. 3 for different values of the uniaxial strain η. A gap correction of 1.07 eV is included, bringing the LDA gap for zero strain 0.48 eV in agreement with the experimental gap of 1.55 eV. We see that at low frequency the birefringence is indeed negative, approximately -0.01 for zero strain, i.e., somewhat less negative than the experimental value of -0.017.[6] One can also see that the variation of birefringence with strain is linear, which is further confirmed by plotting $\Delta n(\omega=0)$ directly as a function of strain in Fig. 4. One finds $\Delta n \approx -0.01 + 1.7\ \eta$.

In the calculations for nonzero strain, we have maintained the internal structural parameter u of the chalcopyrite structure equal to its experimental value for the unstrained situation. We have separately checked with full-potential LMTO calculations that u does not vary significantly with c/a, as is to be expected because it corresponds only to a displacement of the anion sublattice relative to the two types of cation sublattices in planes perpendicular to the c axis. It is basically determined by a balance between the Cd-As and Si-As bondlengths. As already mentioned, the birefringence is not very sensitive to u and, in fact, changing the estimated value of $u=0.2893$ to a FP-LMTO calculated value of $u=0.2866$ had negligible effect. For a 1% strain the u value changed less than 0.0003. The experimental value[6] for the birefringence is -0.017 in fair agreement with our calculation, and shows little dispersion in the midinfrared range except near the band gap.

B. Index of refraction and Sellmeyer parameters

In Fig. 5, we show the calculated indices of refraction for $CdSiAs_2$ as function of wavelength and their fit by means of a Sellmeyer expression[5]

$$n^2 = A + B/(1 - C/\lambda^2) + D/(1 - E/\lambda^2). \qquad (2)$$

The last term in this expression involving the coefficients D and E, is related to the downward curving part of the index of refraction when approaching the long-wavelength region where phonons produce absorption. Since this physics is not included in our first-principles calculation, we fit our data with $D=0$. The resulting Sellmeyer coefficients for $CdSiAs_2$ and $CdSiP_2$ are given in Table II below.

However, the phonon contributions are important and are discussed next. The Sellmeyer equations essentially describe

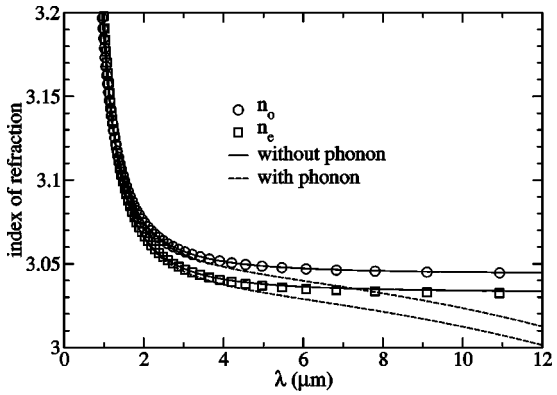

FIG. 5. Calculated indices of refraction for $CdSiAs_2$ (circles for n_o and squares for n_e), a Sellmeyer fit to them (solid lines), and the same with an added "phonon"-related term (dashed lines) responsible for the decrease at long wavelengths.

TABLE I. Phonon data, phonon frequency ν_{TO}, corresponding optical wavelength λ_{TO}, and Sellmeyer parameter E.

	ν_{TO} (cm^{-1})	λ_{TO} (μm)	$(\lambda_{TO})^2$ (μm^2)	E (μm^2)
$ZnGeP_2$	399	25.1	628	660
$CdGeP_2$	384	26.0	676	671
$CdGeAs_2$	272	36.8	1354	1370
$ZnSiAs_2$	405	24.7	610	700
$CdSiP_2$	489	20.4	418	
$CdSiAs_2$	391	25.6[a]	655	

[a]Estimated from Ref. 14 as explained in the text.

the real part of the dielectric function $\varepsilon_1(\omega)$ assuming that its imaginary part simply consists of two poles, one at high frequency, corresponding to band gap aborption and one at low frequency, representing phonon related absorption. In the spirit of the Einstein model for phonons, it seems reasonable to represent the optical phonon spectrum by a single average phonon frequency, which we may identify with, e.g., the TO frequency at the Γ point in the Brillouin zone. There is actually no particular reason to prefer the TO over the LO mode here and to within the accuracy we claim here, either one could serve. From this point of view we expect that the Sellmeyer coefficient E can be identified with λ_{TO}^2. Table I illustrates to what extent this expectation works for some chalcopyrites for which the Sellmeyer parameters have been determined by measurement of the indices of refraction and for which the phonon frequencies are known. We use results from the data compilation of MacKinnon *et al.*[5]

The agreement between the last two columns is reasonably good and in particular shows the remarkable difference between $CdGeAs_2$ from the other materials. Now, the phonon frequencies in $CdSiAs_2$ are not well known but mid infrared absorption data by Averkieva *et al.*[14] indicate a fairly strong absorption peak at about 12.8 μm. By comparison with $CdGeAs_2$ and $ZnGeP_2$ midinfrared absorption data in Ref. 15 it becomes clear that this peak corresponds to a two-phonon process and hence we estimate the λ_{TO} for $CdSiAs_2$ as 25.6 μm. We can thus estimate the E parameters of $CdSiAs_2$ and $CdSiP_2$ to be 660 and 420, respectively.

On the other hand, we note that the strength of the phonon pole or the D parameter does not vary much between the various chalcopyrites and is about 1.5. The effect of adding the terms with D and E can be seen in Fig. 5.

We finally adjust the Sellmeyer A parameter slightly to correct for our underestimate of the individual indices of refraction. This leads us finally to the estimated Sellmeyer parameters given in Table II, in which we also give the indices of refraction that result from them for long wavelength and the calculated strain derivatives. Our calculations for different strains for both $CdSiAs_2$ and $CdSiP_2$ indicate that not only the birefringence but each of the indices n_o and n_e separately vary linearly with strain.

C. Phase matching angles

Having a convenient analytic expression for the indices of refraction, it is then straightforward to obtain the phase matching angle for type-I SHG, i.e., the angle between the optical beam and the optical axis for which the ω and 2ω beams are phase matched, given by

$$\sin^2\theta = \frac{\dfrac{1}{n_o(\omega)^2} - \dfrac{1}{n_o(2\omega)^2}}{\dfrac{1}{\overline{n_e}(2\omega)^2} - \dfrac{1}{n_o(2\omega)^2}} \approx \frac{n_o(2\omega) - n_o(\omega)}{\overline{n_e}(2\omega) - n_o(2\omega)}, \quad (3)$$

where $\overline{n_e}$ is the principal value of the extraordinary index of refraction, i.e., for polarization along the **c** axis. Another process of interest is difference frequency generation. In this case, we are interested in a type-II *eoo* process in which a pump p beam of e polarization of frequency ω gives rise to a signal s and idler i beam both in o polarization of two frequencies which add up to ω. The phase matching equation for this case can be found in Ref. 19 and is given by

$$\sin^2\theta_{PM} = \frac{(n_p^e)^2}{[(\lambda_p/\lambda_s)n_s^o + (\lambda_p/\lambda_i)n_i^o]^2} \times \left(\frac{(n_p^o)^2 - [(\lambda_p/\lambda_s)n_s^0 + (\lambda_p/\lambda_i)n_i^o]^2}{(n_p^o)^2 - (n_p^e)^2} \right). \quad (4)$$

One can also consider the idler as a second pump beam and

TABLE II. Estimated Sellmeyer coefficients, index of refraction, and strain derivative for $CdSiAs_2$ and $CdSiP_2$. The first column gives the A coefficient obtained by fitting to the first-principles calculations and the second column gives the A coefficient slightly adjusted to match the experimental indices and birefringence. The indices n correspond to $\sqrt{A+B}$ using the adjusted value of A. The resulting birefringence Δn and its strain derivative is given separately.

	A (calculated)	A (adjusted)	B	C (μm^2)	D	E(μm^2)	n	$dn/d\eta$
$CdSiAs_2$								
n_o	4.523	6.823	4.742	0.164	1.5	660	3.40	−1.2
n_e	6.071	8.321	3.126	0.245	1.5	660	3.38	0.5
Δn							−0.02	1.7
$CdSiP_2$								
n_o	2.747	6.747	4.784	0.076	1.5	420	3.40	−0.8
n_e	3.162	7.107	4.107	0.086	1.5	420	3.35	1.5
Δn							−0.05	2.3

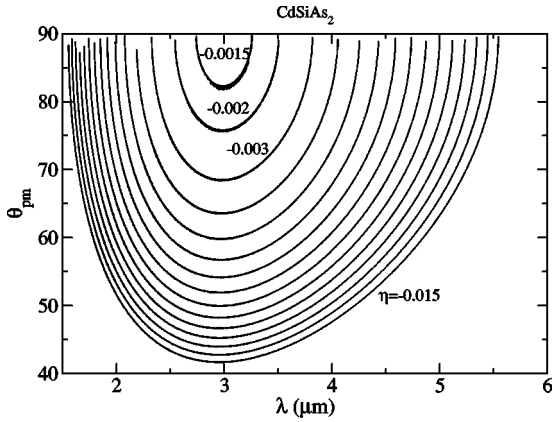

FIG. 6. Phase matching angle θ_{PM} as function of frequency doubled wavelength for $CdSiAs_2$ for different uniaxial strains: $\eta = -0.0015, -0.002, -0.003, \ldots, -0.015$ from innermost to outermost curve.

the signal as the generated difference, although in an optical parametric oscillator (OPO) only a single pump is used and the desired signal is selected by a resonant cavity effect. We note that if $\lambda_s = \lambda_i$, these equations reduce to the one for SHG of signal and idler combining to the pump.

In Fig. 6 we show the results for $CdSiAs_2$ as function of strain. We see that a minimum compressive strain of $\eta = -0.0015$ is required to have any phase matching at all, corresponding to the innermost curve. In fact, for compressive strains smaller than this, the birefringence is simply to small to give any solutions of the Eq. (3) because the dispersion in the midinfrared range is too strong. With increasing strain, the curves move outward. Of particular interest are the wavelengths for which the phasematching angle $\theta_{PM} = 90°$ since this corresponds to NCPM. In particular, we note that CO_2 lasers have a manifold of sharp laser lines in the wavelength range $9-11.5$ μm. This corresponds to $4.5-5.75$ μm for the frequency doubled wave. Thus we can see that a strain of about -0.007 to -0.015 is required to cover this range. On the other hand, if we would frequency double a CO_2 laser line twice, we would need to cover the range 2.25 to 2.75 μm. We see that we can indeed have NCPM again for this purpose now on the left-hand side of the curves with smaller strains of about -0.0015 to -0.0035

One could also use difference frequency generation with a pump near 2 μm (for example, with a Ho-YAG or Tm-YAG laser) and obtain a signal and idler beam both at about 4 μm in an OPO under NCPM conditions. This again would require compressive strains of order -1%. Note, however, that if we consider NCPM, i.e., $\sin \theta_{PM} = 1$, Eq. (4) reduces simply to

$$\omega_1 n^o(\omega_1) + \omega_2 n^o(\omega_2) = (\omega_1 + \omega_2) n^e(\omega_1 + \omega_2). \tag{5}$$

Thus, for a chosen pump frequency $\omega_1 + \omega_2$ and any desired signal frequency $\omega_1 < \omega_{\text{pump}}$, we just have to find the strain such that Eq. (5) is satisfied. Since the birefringence varies linearly with strain, this simply means

$$(\omega_1 + \omega_2)\frac{d\Delta n}{d\eta}\eta = [\omega_1 n^o(\omega_1) + \omega_2 n^o(\omega_2) - (\omega_1 + \omega_2) n^e(\omega_1 + \omega_2)]_{\eta=0}, \tag{6}$$

where the right-hand side can be evaluated straightforwardly using the data from Table II. For example, by pumping with 2 μm light, one could generate a signal and idler of wavelengths 6 and 3 μm. In that case $n^o(\omega_1) = 3.4106$, $n^o(\omega_2) = 3.3912$, $n^e(\omega_1 + \omega_2) = 3.4120$ and a the strain required for NCPM is -0.0046.

The questions is now if strains of this magnitude are achievable. To this purpose, we calculated the elastic constant for uniaxial deformation along the **c** axis, which can be expressed in terms of the elastic constants for a tetragonal crystal with point group $\bar{4}2\,m$ as follows:

$$C_{[001]} = (2C_{33} - C_{11} - C_{12})/2, \tag{7}$$

by evaluating the curvature of the energy (per unit volume) u versus strain η curve

$$u = \frac{1}{2} C_{[001]} \eta^2. \tag{8}$$

This is done using the FP-LMTO method mentioned earlier and gives a value of 27 GPa, which seems reasonable in comparison with elastic constants of for example GaAs. In that case, the corresponding elastic constant would be $(C_{11} - C_{12})/2$ which evaluates to 28 GPa using measured elastic constants reported in the Landolt-Börnstein tables.[16] This means that a 1% compressive strain requires a stress of about 0.3 GPa. This is fairly large but not impossible to achieve. For example, in studies of uniaxial deformation potentials of semiconductors, one uses stresses up to 1 GPa.[7]

For OPO and SHG applications, one typically works with bulk crystals because one needs to perform angular tuning. However, under NCPM conditions, one might consider using a thin film geometry since the beam would propagate in the direction perpendicular to the **c** axis and thus in the film (conventionally grown normal to the **c** axis). Fairly high strains can be obtained in thin films by growing a film on a mismatched substrate and thus putting it under biaxial strain. For a 1% compressive uniaxial strain, roughly a 0.5% biaxial tension is required. However, the achievable strains in this way are usually significantly smaller, except in films of only a few atomic layers, because of the generation of misfit dislocations which relax the strain. Nevertheless, it might be possible to achieve the required strains simply by bending the substrate on which the thin film is deposited and making sure the beams follow the film by confining them within a waveguide. Small adjustments of the c/a might also be possible by temperature tuning, since $CdSiP_2$ and related chalcopyrites have a strongly anisotropic linear thermal expansion. [5]

Alloying with $CdSiP_2$ to make the birefringence more negative is an alternative solution to tune the birefringence. Linear dependence of the indices of refraction on alloy composition is not obvious, but is a frequently made assumption in the field.[1] A systematic verification of the linear dependence on alloy composition would require one to model ran-

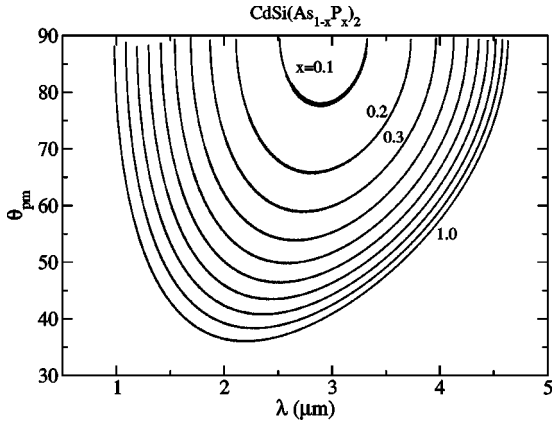

FIG. 7. Phase matching angle θ_{PM} as a function of frequency doubled wavelength for $CdSi(As_{1-x}P_x)_2$ for $x=0.1-1$, the innermost curve corresponding to $x=0.1$.

dom alloys, which is beyond the scope of this paper. However, it is easily verified that the assumption of linear dependence of the indices of refraction gives similar results to the assumption of linear variation of the Sellmeyer coefficients, another plausible assumption. Assuming linear variation of the indices of refraction with composition and using the parameters of Table II we obtain the results shown in Fig. 7.

We can see that with increasing concentration of *P* the range of wavelengths for which phase matching is possible increases. We also see that for pure $CdSiP_2$ NCPM for SHG occurs for optical wavelengths of the 2ω beam at 4.6 μm, or the fundamental at $\lambda=9.2$ μm, i.e., at the lower end of the CO_2 laser frequencies. To achieve NCPM SHG of longer wavelengths one would need to increase the birefringence, which again would be possible by compressive strain along the c axis. NCPM OPO applications with pumps at about 1 μm would also be possible for pure $CdSiP_2$, e.g., using the popular Nd-YAG laser at 1.064 μm.

D. Nonlinear optical coefficients

Having demonstrated the feasibility of phase matching for $CdSiAs_2$ under strain and for $CdSiP_2$ and $CdSi(P_xAs_{1-x})_2$ alloys we now consider the $\chi^{(2)}$ and the SHG figure of merit[18,19] (FOM) $[\chi^{(2)}]^2/n^3$ in comparison with other chalcopyrite semiconductors in Table III. The figure of merit is chosen based on the fact that for SHG, the efficiency $\eta = P_{2\omega}/P_{\omega}$ for perfect phase matching is given by[19]

$$\eta = \frac{8\pi^2 d_{\text{eff}}^2 L^2 I_{\omega}}{\varepsilon_0 n_{\omega}^2 n_{2\omega} c \lambda_{\omega}^2}, \tag{9}$$

in SI units and where $d_{\text{eff}}=\frac{1}{2}\chi_{\text{eff}}^{(2)}$, L is the path length the beam traverses through the crystal, I_{ω} is the intensity of the input beam, and λ_{ω} is the wavelength of the input beam. The NLO coefficients are taken from our previous calculations[2,3] and the other properties from the Landolt-Börnstein tables.[5]

In this table, $CdSiAs_2$ has the second highest $\chi^{(2)}$. This high value of $\chi^{(2)}$, is in fact, due to the very small negative purely interband contribution to $\chi^{(2)}$, such that the large positive mixed intraband-interband contribution dominates. As discussed in Ref. 2, this is in contrast with the usual behavior of the two contributions which in most chalcopyrites cancel to a large extent. $CdSiAs_2$ shares this unusual property with $CdGeAs_2$. Although $CdGeAs_2$ has a much smaller phase-matching angle of about 33.57° for CO_2 frequency doubling,[20] it should be kept into account that for a positive birefringent material the effective $\chi_{\text{eff}}^{(2)}=\chi_{zxy}^{(2)}\sin 2\theta$ for an *eeo* process and hence $CdGeAs_2$ still seems to have a superior $\chi_{\text{eff}}^{(2)}$ than $CdSiAs_2$ even without NCPM. On the other hand, the actual value of the $\chi^{(2)}$ of $CdGeAs_2$ is still somewhat uncertain and the theoretical value used here may be a bit optimistic. This is because the band gap in $CdGeAs_2$ is very small and in fact negative in LDA (Ref. 17) and hence the calculated $\chi^{(2)}$ is more sensitive to the way in which one corrects for the LDA band gap underestimate than in other materials. However, $CdGeAs_2$ has the disadvantage that NCPM cannot be used and hence it is subject to the walk-off problem. Compared with $AgGaSe_2$, $CdSiP_2$ has the advantage of NCPM for desired wavelengths and has a competitive $\chi^{(2)}$ and may have a higher thermal conductivity. However, the $AgGaSe_2$ and telluride have probably advantages in terms of transparency range.

TABLE III. Comparison of NLO properties for different chalcopyrites. The experimental values of the band gap E_{gap} and birefringence Δn are taken from Refs. 5 and 6 the calculated $\chi^{(2)}$ values are from Refs. 2 and 3 and the experimental values between parentheses are from various sources quoted in the same papers where the theoretical values are taken from.

	E_{gap} (ev)	$\chi^{(2)}$ (pm/V)	Δn	$[\chi^{(2)}]^2/n^3$
$CdSiP_2$	2.45	73	−0.051	135
$CdSiAs_2$	1.55	139	−0.017	700
$CdGeAs_2$	0.65	506(351−472)	0.110	5450
$ZnGeP_2$	2.05	102(111−150)	0.039	330
$AgGaS_2$	2.64	26(18−23)	−0.055	50
$AgGaSe_2$	1.80	66(64−68)	−0.033	250
$AgGaTe_2$	1.32	138	0.016	730

Indeed, another consideration for nonlinear optical applications is the transparency range. On the short wavelengths side this is determined by the band gap. The band gaps of $CdSiP_2$ and $CdSiAs_2$ are sufficiently large to allow for pumping with about 1 μm lasers, which gives them an advantage over $CdGeAs_2$ for those applications. At the long wavelength side, the transparency is usually limited by the position of the multiphonon lines. In particular, the optical absorption corresponding to two phonon generation tend to be rather strong and may limit applications for $CdSiP_2$, because the latter has a fairly high phonon frequency because of the light P and Si atoms. In fact, the optical wavelength corresponding to a two phonon process is about 10 μm which overlaps with the CO_2 frequency range. Even three phonon processes are found to limit applications of $ZnGeP_2$ for CO_2 doubling because they occur at 8.3 μm. Interestingly, the mid infrared absorption data from Averkieva *et al.*[14] do not show a three-phonon absorption band for $CdSiAs_2$ and the two-phonon absorption

band occurs at 12.8 μm, i.e., beyond the CO_2 laser line manifold. Thus $CdSiAs_2$ under compressive strain of about 1% may be suitable for CO_2 frequency doubling as well as for OPO applications with pumps near 2 μm.

IV. CONCLUSION

In conclusion, our calculations indicate that both $CdSiAs_2$ and $CdSiP_2$ are II-IV-V_2 chalcopyrite materials with significant potential for NLO frequency conversion applications. Their negative birefringence opens the way towards design of noncritically phase matched materials by strain (and temperature) tuning or by alloying between these two compounds for various processes leading to wavelengths in the midinfrared, such as optic parametric oscillators with pumping by lasers at about $1-2$ μm or CO_2 laser SHG. Our calculations confirmed the negative birefringence of both $CdSiAs_2$ and $CdSiP_2$. The actual calculated values were to within 0.01 of the experimental values but furthermore indicate the strong sensitivity of the birefringence to uniaxial strain. A strain coefficient $d\Delta n/d\eta$ of about 2 was obtained for both materials, indicating that with a strain of order 0.01 a significant change in birefringence can be realized.

While from the NLO coefficient point of view $CdSiAs_2$ is much more desirable than $CdSiP_2$ (about a factor 2 larger $\chi^{(2)}$) its negative birefringence is slightly too small to overcome the fairly large dispersion in the midinfrared. We showed that even in the absence of index of refraction measurements, we can estimate the midinfrared dispersion of the index of refraction from a knowledge of the optical phonon frequencies combined with our calculated data. We suggest that the too low birefringence in $CdSiAs_2$ could be overcome by uniaxial compression. Our calculations show that the strain coefficient of the birefringence both in $CdSiP_2$ and $CdSiAs_2$ is of order 2, which is fairly large and allows for tuning over the relevant range with uniaxial strains of the order of 1%. This is not trivial but should be feasible with currently available stress apparatus since it requires stresses less than 1 GPa and by exploiting the fact that under NCPM conditions thin films could be utilized instead of bulk crystals.

ACKNOWLEDGMENTS

This work was supported by the Air Force Office of Scientific Research under Grant No. F49620-03-1-0010. It is a pleasure to thank Dr. G. Medvedkin for pointing us to the experimental data on $CdSiAs_2$.

[1] M. C. Ohmer, J. T. Goldstein, D. E. Zelmon, A. W. Saxler, S. M. Hegde, J. D. Wolf, P. G. Schunemann, and T. M. Pollak, J. Appl. Phys. **86**, 94 (1999).

[2] S. N. Rashkeev, S. Limpijumnong, and W. R. L. Lambrecht, Phys. Rev. B **59**, 2737 (1999).

[3] S. N. Rashkeev and W. R. L. Lambrecht, Phys. Rev. B **63**, 165212 (2001).

[4] G. C. Catella and D. Burlage, MRS Bull. **23**, 28 (1998).

[5] A. MacKinnon, in *Landolt-Börnstein Numerical Data and Functional Relationships in Science and Technology*, New Series, Group III, *Crystal Solid State Physics* Vol. 17, *Semiconductors*, Subvolume h, *Physics of Ternary Compounds*, edited by O. Madelung (Springer, Berlin, 1985).

[6] A. S. Borshchevskii, V. S. Grigoréva, Yu. K. Undalov, and T. P. Upatova, Fiz. Tekh. Poluprovod. **6**, 396 (1972) [Sov. Phys. Semicond. **6**, 338 (1972)].

[7] L. D. Laude, F. H. Pollak, and M. Cardona, Phys. Rev. B **3**, 2623 (1971).

[8] O. K. Andersen, O. Jepsen, and M. Šob, in *Electronic Band Structure and Its Applications*, edited by M. Yussouff (Springer, Heidelberg, 1987), p. 1.

[9] L. Hedin and B. I. Lundqvist, J. Phys. C **4**, 2064 (1971).

[10] W. R. L. Lambrecht, B. Segall, J. Rife, W. R. Hunter, and D. K. Wickenden, Phys. Rev. B **51**, 13 516 (1995).

[11] Z. H. Levine and D. C. Allan, Phys. Rev. Lett. **63**, 1719 (1989).

[12] N. Itoh, T. Fujinaga, and T. Nakau, Jpn. J. Appl. Phys. **17**, 951 (1978).

[13] M. Methfessel, M. van Schilfgaarde, and R. A. Casali, in *Electronic Structure and Physical Properties of Solids, The Uses of the LMTO Method*, edited by Hugues Dreyssé, Springer Lecture Notes, Workshop Mont Saint Odille, France, 1998 (Springer, Berlin, 2000), pp. 114–147.

[14] G. K. Averkieva, R. V. Larymshakov, V. D. Prochukhan, and M. Serginov, Fiz. Tekh. Poluprov. **4**, 591 (1970) [Sov. Phys. Semicond. **4**, 494 (1970)].

[15] P. G. Schunemann and T. M. Pollak, MRS Bull. **23**, 23 (1998).

[16] *Landolt-Börnstein Tables of Numerical Data and Functional Relationships in Science and Technology*, New Series, *Intrinsic Properties of Group IV Elements, and III-VI, II-VI, and I-VII Compounds*, Group III, Vol. 22a, edited by O. Madelung (Springer, Berlin, 1987).

[17] S. Limpijumnong and W. R. L. Lambrecht, Phys. Rev. B **65**, 165204 (2002).

[18] A. G. Jackson, M. C. Ohmer, and S. R. LeClair, Infrared Phys. Technol. **38**, 233 (1997).

[19] R. L. Sutherland, *Handbook of Nonlinear Optics* (Marcel Dekker, New York, 1996).

[20] V. G. Dmitriev, G. G. Gurzadya, and D. N. Nikogosyan, *Handbook of Nonlinear Optical Crystals*, 3rd revised ed., Vol. 64 of Springer Series in Optical Sciences, edited by A. E. Siegman (Springer-Verlag, Berlin, 1999), p. 176.